10

Tungsten Isotopes and the Origin of Chondrules and Chondrites

THORSTEN KLEINE, GERRIT BUDDE, JAN L. HELLMANN, THOMAS S. KRUIJER, AND CHRISTOPH BURKHARDT

Abstract

Chondrules and matrix from carbonaceous chondrites exhibit complementary nucleosynthetic W isotope anomalies that result from the depletion of a metallic *s*-process carrier in the chondrules, and the enrichment of this carrier in the matrix. The complementarity is difficult to reconcile with an origin of chondrules in protoplanetary impacts and also with models in which chondrules and matrix formed independently of each other in distinct regions of the disk. Instead, the complementarity indicates that chondrules formed by localized melting of dust aggregates in the solar nebula. The Hf–W ages for metal-silicate fractionation in CV and CR chondrites are 2.2 ± 0.8 Ma and 3.6 ± 0.6 Ma after formation of Ca-Al-rich inclusions, and are indistinguishable from Al–Mg ages for CV and CR chondrules. The good agreement between these ages strongly suggests that ^{26}Al was homogeneously distributed in the solar protoplanetary disk and that therefore Al–Mg ages are chronologically meaningful. The concordant Al–Mg and Hf–W ages reveal that chondrule formation (as dated by Al–Mg) was associated with metal-silicate fractionation (as dated by Hf–W), both within a given chondrite but also among the different subgroups of ordinary chondrites. These age data indicate that chondrules from a given chondrite group formed in a narrow time interval of <1 Ma, and that chondrule formation and chondrite accretion were closely linked in time and space. The rapid accretion of chondrules into a chondrite parent body is consistent with the isotopic complementarity, which requires that neither chondrules nor matrix were lost prior to chondrite accretion. Combined, these observations suggest that chondrule formation was an important step in the accretion of planetesimals.

10.1 Introduction

Chondrules are the major component of most chondrites, and judging by their abundance, must have formed by one of the most common processes in the early solar system. The nature and timing of this process remain poorly understood, however. The different formation hypotheses that have been proposed for the origin of chondrules can be divided into two general categories (e.g., Connolly and Desch, 2004): those in which chondrules formed by melting of dust in the solar protoplanetary disk (the solar nebula) and those in which chondrules formed during protoplanetary impacts. Distinguishing between these distinct models is important not only for understanding the origin of chondrules, but also for assessing the role chondrule formation might have played in planet formation. If chondrules formed by melting of dust aggregates

within the disk, followed by rapid accretion into a parent body, their formation may have been important for mediating the accumulation of dust into planetesimals. If, however, chondrules formed by protoplanetary impacts, then they would merely be a by-product of planet formation.

Studies aimed at identifying the chondrule-forming process typically focus on reproducing the properties of chondrules, but often ignore the other major components of chondrites, namely fine-grained matrix and metal. However, these three components seem to be genetically linked. For instance, chondrules and matrix in carbonaceous chondrites have complementary chemical compositions, suggesting that chondrules and matrix from a given chondrite group formed from a single reservoir of precursor dust (Bland et al., 2005; Hezel and Palme, 2008; Hezel and Palme, 2010; Palme et al. 2015; Ebel et al., 2016; Chapter 4). Further, metal in primitive chondrites predominantly seems to have been reprocessed or newly formed during chondrule formation (Zanda et al., 1994; Connolly et al. 2001; Campbell et al., 2005), meaning that chondrules and metal are probably also genetically linked. Thus, any successful model for the origin of chondrules must not only identify the chondrule-forming process, but must also account for the formation of matrix and metal, and the subsequent accretion of all three components to a chondrite parent body.

In this chapter, we review how the W isotopic compositions of chondrules, matrix, and metal from primitive (unmetamorphosed) chondrites help to shape models of chondrule formation and chondrite accretion. In particular, we will discuss how the W isotopic data can distinguish between an impact and solar nebula origin of chondrules, and review the Hf–W chronology of chondrule formation and metal-silicate fractionation in chondrites. Finally, we compare the Hf-W ages to results obtained from other chronometers, with the ultimate goal to establish a coherent timescale of chondrule formation and chondrite parent body accretion.

10.2 Tungsten Isotope Systematics

Tungsten isotope variations can be nucleosynthetic, radiogenic, or cosmogenic in origin (Kleine and Walker, 2017). *Cosmogenic* W isotope variations result from the interaction with cosmic rays and predominantly occur in iron meteorites and lunar samples. For chondrites and their components, cosmogenic effects on W isotopes are not important and will therefore not be discussed here. *Nucleosynthetic* W isotope variations arise through the heterogeneous distribution of isotopically distinct presolar materials, and are powerful tracers to assess genetic links between meteoritic and planetary materials. *Radiogenic* W isotope variations result from the decay of short-lived ^{182}Hf to ^{182}W with a half-life of 8.9 million years (Ma) and form the basis of the Hf–W chronometer to date early solar system processes.

10.2.1 Nucleosynthetic W Isotope Variations

The heterogeneous distribution of isotopically distinct presolar materials leads to correlated variations of ^{182}W/^{184}W and ^{183}W/^{184}W (Burkhardt et al., 2012; Figure 10.1). Such nucleosynthetic W isotope variations can be used to assess genetic links between meteoritic materials, because the heterogeneous distribution of presolar material between two genetically linked components leads to complementary W isotope anomalies relative to the bulk material.

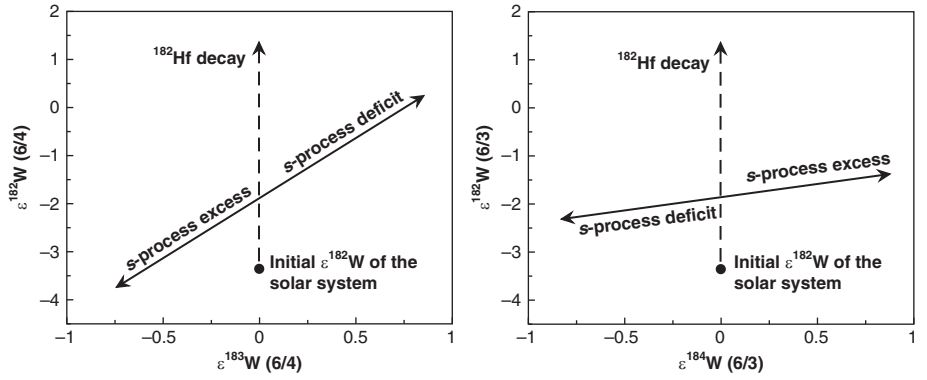

Figure 10.1 Schematic illustration of W isotope variations. Tungsten isotope ratios are shown in ε-units, corresponding to the deviation from terrestrial standard values in part per 10,000. (6/4) and (6/3) stand for normalization of the W isotope ratios to a fixed $^{186}W/^{184}W$ or $^{186}W/^{183}W$, respectively.

Nucleosynthetic isotope variations predominantly affect W isotope ratios involving ^{184}W, and so measurements of $^{183}W/^{184}W$ (when internally normalized to $^{186}W/^{184}W$) are ideally suited to quantify the extent of nucleosynthetic W isotope heterogeneity. By contrast, the $^{182}W/^{183}W$ ratio (when internally normalized to $^{186}W/^{183}W$) shows only small nucleosynthetic variations (Figure 10.1). This is because ^{184}W has the largest contribution from the *s*-process of stellar nucleosynthesis, while ^{182}W, ^{183}W and ^{186}W have similar *s*-process contributions (Arlandini et al., 1999; Qin et al., 2008b; Burkhardt et al., 2012). Thus, the heterogeneous distribution of *s*-process matter affects ^{182}W, ^{183}W, and ^{186}W almost equally, resulting in only small changes of the $^{182}W/^{183}W$ ratio. These small changes can be reliably corrected, meaning that the presence of nucleosynthetic W isotope anomalies does not compromise the use of the ^{182}Hf–^{182}W chronometer.

10.2.2 ^{182}Hf–^{182}W Chronometer

The ^{182}Hf–^{182}W chronometer can be used for dating processes that occurred in the first ~60 Ma of the Solar System (Kleine et al., 2009; Kleine and Walker, 2017). There are several properties that distinguish the Hf–W system from other chronometers typically utilized for dating chondrule formation, such as the ^{26}Al–^{26}Mg and ^{207}Pb–^{206}Pb systems. First, the Hf–W system does not directly provide crystallization ages for individual chondrules, but instead provides the timing of Hf–W fractionation among chondrite components. As Hf is lithophile, but W siderophile, the dominant process fractionating Hf from W is metal-silicate fractionation. Chondrules are typically enriched in refractory lithophile and depleted in siderophile elements, whereas matrix displays the complementary depletions and enrichments (e.g., Palme et al., 2015). Moreover, metal in primitive chondrites predominantly seems to have formed or was reprocessed during chondrule formation (e.g., Campbell et al., 2005). These observations combined reveal that chondrules, matrix, and metal have different Hf/W ratios, most likely as a result of metal-silicate fractionation during chondrule formation, making it possible to date chondrule formation using the Hf–W system.

Another important property of the Hf–W system is its high closure temperature of typically 800–900 °C (Kleine et al., 2008), making it more robust against thermal resetting than the Al–Mg and Pb–Pb systems (e.g., the closure temperature for Al–Mg in anorthite is <600 °C; Van Orman et al., 2014). Finally, ^{182}Hf was homogeneously distributed within the solar protoplanetary disk, and so unlike for ^{26}Al there is no doubt that variations in initial ^{182}Hf/^{180}Hf ratios reflect time differences rather than distinct formation locations within the disk (Kleine et al., 2009).

A Hf–W isochron for chondrites is typically defined by data for chondrule or silicate fractions and matrix or metal. The age of a sample is then obtained from the slope of the isochron, which provides the ^{182}Hf/^{180}Hf at the time of Hf–W closure. The Hf–W ages are expressed as the time elapsed since formation of Ca-Al-rich inclusions (CAIs), generally thought to represent the first solids formed in the solar system:

$$t_{CAI} = -\frac{1}{\lambda} \times ln\left(\frac{^{182}Hf/^{180}Hf_{sample}}{^{182}Hf/^{180}Hf_{CAI}}\right)$$

where the initial ^{182}Hf/^{180}Hf of CAIs is $(1.018 \pm 0.043) \times 10^{-4}$, as defined by a Hf–W isochron for CAIs (Burkhardt et al., 2008; Kruijer et al., 2014a), and $\lambda = 0.078 \pm 0.002$ Ma^{-1} (Vockenhuber et al., 2004).

In summary, W isotope variations among chondrules and other components of primitive chondrites can be used not only for dating the formation of chondrite components, but also for assessing potential genetic links among them. This combination of constraining both the genetic heritage and age of a sample makes W isotopes a uniquely powerful tool for investigating the origin of chondrules and chondrites.

10.3 Isotopic Complementarity and the Origin of Chondrules

10.3.1 Complementary Nucleosynthetic Isotope Anomalies in Chondrules and Matrix

Chondrule and matrix samples from the Allende CV3 chondrite exhibit nucleosynthetic ^{183}W anomalies that are indicative of an *s*-process deficit (or *r*-excess) in chondrules and a complementary *s*-excess (or *r*-deficit) in matrix (Figure 10.2) (Budde et al., 2016b). The same Allende chondrules and matrix samples also exhibit complementary Mo isotope anomalies[1] (Figure 10.3) (Budde et al., 2016a). Of note, the Mo and W isotope anomalies are broadly correlated, suggesting strongly that they result from the heterogeneous distribution of the same presolar carrier. Unlike for W, the Mo isotopic data can be used to distinguish between *s*- and *r*-process heterogeneity and, as such, make it possible to determine whether a presolar carrier is enriched in matrix and depleted in chondrules or vice versa. As the Mo isotope variations

[1] Complementarity is strictly defined as complementary compositions of two components relative to a well-defined bulk composition (see Chapter 4). The prerequisite of a well-defined bulk composition is met for ^{183}W, because bulk meteorites as well as the Earth, Mars, and Moon have very similar ^{183}W compositions, in contrast to the large ^{183}W anomalies observed for chondrules and matrix. For Mo isotopes, the situation is different because bulk meteorites exhibit large Mo isotope variations. Thus, although the Mo isotope anomalies in chondrules and matrix reflect the complementary depletion and enrichment of a single *s*-process carrier, these anomalies are *not* complementary relative to a common bulk composition.

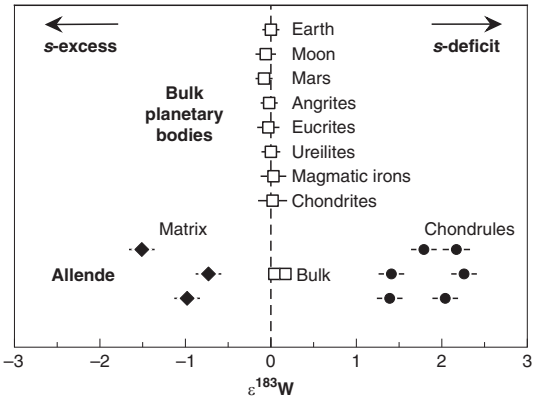

Figure 10.2 Complementary $\varepsilon^{183}W$ compositions for Allende chondrules and matrix. Bulk meteorites show no or only small $\varepsilon^{183}W$ anomalies. W isotopic data from Budde et al. (2016b) and references therein.

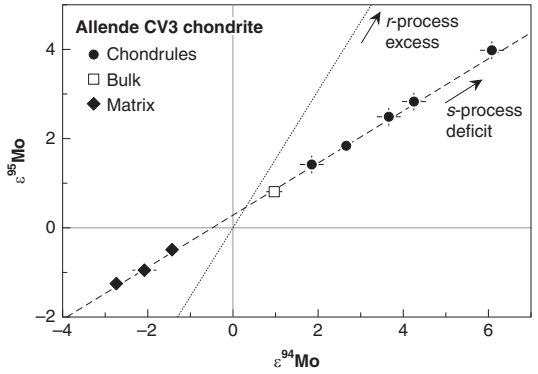

Figure 10.3 Complementary Mo isotopic anomalies for Allende chondrules and matrix. Data are given in ε-units, as the parts per 10,000 deviations of $^{95}Mo/^{96}Mo$ and $^{94}Mo/^{96}Mo$ ratios from terrestrial standard values. The chondrule and matrix samples plot along a mixing line (dashed line) between presumed *s*-process enriched and depleted end member compositions; the heterogeneous distribution of *r*-process matter would have resulted in different Mo isotope anomalies, as indicated by the dotted line. Data from Budde et al. (2016a).

among chondrules and matrix reflect the heterogeneous distribution of an *s*-process carrier (Figure 10.3), these data therefore indicate that chondrules are depleted, whereas matrix is enriched in this carrier (Budde et al., 2016a). By contrast, the heterogeneous distribution of an *r*-process carrier would have led to different Mo isotope signatures, most notably larger ^{95}Mo anomalies for a given ^{94}Mo anomaly (Figure 10.3). It is noteworthy that the different chondrule separates display variable Mo and W isotope anomalies (Figures 10.2 and 10.3), indicating variable depletions of the *s*-process carrier in the chondrules. As each of these separates consists of several hundreds to thousands of chondrules, the isotopic variability among the chondrule separates also implies that there are even larger Mo and W isotope anomalies in individual chondrules.

Unlike for W and Mo, the chondrule and matrix samples do not show complementary isotope anomalies for Ba (Budde et al., 2016a) and Ti (Gerber et al., 2017). Thus, isotopic complementarity only seems to exist for siderophile (Mo, W), but not lithophile (Ba, Ti), elements. This, and the observation that the Mo (and W) isotope anomalies in different chondrule separates are correlated with magnetic susceptibility (and hence initial metal content), indicates that the nucleosynthetic isotope variations result from the heterogeneous distribution of a metallic presolar carrier (Budde et al., 2016a). Thus, Allende chondrules are variably depleted in a presolar metal enriched in *s*-process Mo and W nuclides, and this same carrier is enriched in the matrix.

As discussed in Budde et al. (2016a, 2016b), several lines of evidence indicate that the Mo and W isotope anomalies are not the result of parent body alteration. First, the isotope anomalies cannot reflect the liberation and redistribution of Mo and W from isotopically anomalous CAIs, because most CAIs have smaller ^{183}W anomalies than chondrules and because CAIs only exhibit ^{183}W excesses but no deficits (Burkhardt et al., 2008; Kruijer et al., 2014a). As such, neither the large ^{183}W excesses in chondrules nor the ^{183}W deficits in matrix can be explained in this manner. Moreover, whereas the isotope anomalies in most CAIs result from an excess in *r*-process nuclides, the anomalies in chondrules and matrix reflect heterogeneity in an *s*-process carrier (note that *r*- and *s*-process heterogeneity results in very different Mo isotope patterns). Thus, the isotope anomalies observed in CAIs are of different origin than those observed in chondrules and matrix. Second, chondrules are characterized by a deficit in *s*-process isotopes, meaning that to account for this composition by parent body alteration would require the removal of a presolar *s*-process carrier from the solidified chondrules. However, as igneous objects, chondrules contain no presolar grains. Thus, the complementary isotope anomalies in chondrules and matrix cannot be the result of parent body processes, but must have been established during the formation of these two components.

10.3.2 Genetic Link between Chondrules and Matrix

The isotopic complementarity of chondrules and matrix implies that both components are genetically linked and must therefore have formed from the same reservoir of dust. This conclusion arises from several observations. First, the isotope anomalies reflect the heterogeneous distribution of a single *s*-process carrier, which is most easily explained by a *single* process in which chondrules became depleted, and matrix enriched in the very same presolar *s*-process carrier. Second, in spite of the large ^{183}W anomalies in chondrules and matrix, bulk meteorites, including Allende, show no or only very small ^{183}W anomalies. Thus, chondrules and matrix are mixed in exactly the right proportions so that *no* ^{183}W anomaly is produced in the bulk chondrite. It would take extraordinary circumstances to accomplish this by random mixing of chondrules and matrix that formed independently of each other. Instead, formation of chondrules and matrix with their large and complementary ^{183}W anomalies from a single reservoir having the average ^{183}W composition of the inner solar system (as defined by bulk meteorites, Earth, and Mars) naturally leads to a bulk chondrite with *no* ^{183}W anomaly, provided that neither chondrules nor matrix were lost (Figure 10.2).

Finally, the nucleosynthetic W (and Mo) isotope anomalies of chondrules and matrix are larger than those observed for any bulk meteorite (Figure 10.2). Moreover, the matrix is

characterized by an excess in *s*-process nuclides, unlike the compositions observed for any bulk meteoritic or planetary material. As such, the nucleosynthetic isotope anomalies in chondrules and matrix cannot represent signatures of distinct formation regions in the disk[2], but must reflect processes that occurred during chondrule formation itself.

10.3.3 Implications for the Origin of Chondrules

The isotopic complementarity of chondrules and matrix is a fundamental observation that is key for constraining the origin of chondrules. Any successful model for chondrule formation must therefore provide (*i*) a mechanism for generating the complementary isotope anomalies, (*ii*) a process by which chondrules and matrix derive from the same reservoir of dust, and (*iii*) a process by which chondrules and matrix were accreted into a parent body in their original proportions, that is in the correct proportion to *not* produce a ^{183}W anomaly in the bulk chondrite. Below we evaluate to what extent existing models for the origin of chondrules are consistent with these requirements.

Impact models for the origin of chondrules have great difficulty in meeting the constraints provided by the isotopic complementarity. In its original form, the impact model posits that chondrules originated as 'splashes' expelled by the collision of molten planetesimals (Zook, 1981; Asphaug et al., 2011; Sanders and Scott, 2012). Support for this model comes from the observation that the parent bodies of differentiated meteorites accreted earlier than the chondrite parent bodies (Kleine et al., 2005; Scherstén et al., 2006; Qin et al., 2008a; Kruijer et al., 2014b 2017), implying that differentiated and probably still molten bodies were present at the time of chondrule formation. However, chondrules exhibit larger nucleosynthetic Mo and W isotope anomalies than observed for bulk, differentiated meteorites (Figure 10.2). Thus, even though differentiated bodies were present, melt splashes from these bodies cannot represent the material from which chondrules ultimately formed. Moreover, the splashing model does not provide a mechanism for producing nucleosynthetic isotope anomalies in the matrix. In this model, matrix either represents primordial dust from the solar nebula or derives from the regolith of the colliding planetesimals (e.g., Sanders and Scott, 2012). However, in both cases the matrix would not be expected to have nucleosynthetic isotope anomalies relative to bulk meteorites and would also not be expected to exhibit complementary isotope anomalies relative to chondrules.

In a recent modification of the splashing model, now termed the 'dirty plume' model (Chapter 14), it is proposed that within the impact plume the melt droplets mixed with primitive dust (containing presolar grains), and that during this mixing an *s*-process carrier was preferentially incorporated into the matrix and not included into the melt droplets that then became chondrules. In this model, the ^{183}W excesses in the chondrules would reflect the contamination of isotopically normal melt droplets with primitive dust that is characterized by large ^{183}W excesses. Such large excesses could in principle exist in presolar grains enriched in *r*-process nuclides. As argued above, however, the nucleosynthetic isotope anomalies in the

[2] Note that Zanda et al. (Chapter 5) suggest that the isotopic complementarity indicates that chondrules and matrix formed in distinct areas of the disk. As outlined here, however, this cannot be correct.

chondrules do not reflect addition of an *r*-process carrier but result from the removal of an *s*-process carrier. Moreover, mass balance indicates that ^{183}W excesses of dust grains resulting from the removal of an *s*-process carrier would not be very large because only a very small fraction of the bulk W is removed. Consequently, large amounts of *s*-process-depleted dust grains would need to be added to the melt droplets to produce the ^{183}W excesses in the final chondrules. Adding such large amounts of material to the melt droplets, while at the same time specifically excluding an *s*-process carrier from this material, seems highly unlikely.

Other versions of the impact model invoke collisions of planetesimals that are either undifferentiated or maintained a primitive, unmelted crust (e.g., Chapter 13). In this model, chondrules originate from the melt produced by impact jetting. This model is, nonetheless, also difficult to reconcile with the constraints from isotopic complementarity. First, there is no *a priori* reason why the impact melting should have produced melt droplets that are variably depleted in a presolar *s*-process carrier. Second, and most importantly, these melt droplets would have to be remixed with primitive dust (i.e., the matrix) that contained the complementary proportion of this *s*-process carrier to yield the original and nearly constant W isotopic composition of bulk chondrites and inner solar system planets (Figure 10.2). To meet this requirement, the melt droplets that ended up as chondrules in the final chondrite, and the source material from which these melt droplets originally derived (i.e., the material that became the matrix), must be sampled in an unbiased way, because otherwise the final chondrule-matrix mixture would not have the ^{183}W composition of bulk inner solar system planets. However, it seems quite unlikely that the original proportion of chondrules and matrix could be retained throughout the impact melting and subsequent ejection and accretion of material. This example, as well as the example of the dirty plume model discussed above, illustrate that attempting to account for the isotopic complementarity of chondrules and matrix adds substantial complexity to impact models.

The *x*-wind model for the origin of chondrules (Shu et al., 1996) (or any other model that invokes transport of chondrules over wide distances in the disk) also is difficult to reconcile with the isotopic complementarity of chondrules and matrix. In this model, chondrules originated near the Sun and were then transported outwards by several astronomical units (AU) to fall back onto the protoplanetary disk, where they were mixed with primitive dust (i.e., the matrix). However, the random mixing of chondrules and matrix predicted in the *x*-wind model is inconsistent with the observation that in spite of the large ^{183}W anomalies in chondrules and matrix, bulk chondrites have no significant ^{183}W anomalies (Figure 10.2). Moreover, the *x*-wind model provides no mechanism for generating isotope anomalies in chondrules and matrix, because these anomalies are unlike those observed for bulk meteorites and, hence, not a signature of distinct formation regions in the disk (see above). Of note, nucleosynthetic isotope anomalies in bulk meteorites reveal that material formed at greater heliocentric distance exhibits a larger *s*-process deficit than material formed closer to the Sun (Burkhardt et al., 2011; Render et al., 2017). In the *x*-wind model, matrix should therefore exhibit an *s*-process deficit compared to chondrules. However, matrix is characterized by an excess, not a deficit, in *s*-process matter.

In contrast to the *x*-wind and impact models, an origin of chondrules by localized melting of dust aggregates in the solar nebula (e.g., Connolly and Desch, 2004) can readily account for the

isotopic complementarity observed. This is because such models provide viable mechanisms for generating the complementary distribution of presolar grains between chondrules and matrix, and they also allow for keeping matrix and chondrules together. For instance, the complementary isotope anomalies could have been produced by metal-silicate fractionation during chondrule formation, which may have resulted in the preferential incorporation of a presolar metal enriched in *s*-process matter into the chondrite matrix. Alternative options include the sorting of dust grains according to their size or magnetic properties. For instance, the enhanced sticking properties of magnetized Fe-metal bearing dust grains could lead to their settling to the midplane of the disk, preferentially removing metal from the precursor dust of chondrules (Hubbard, 2016a, 2016b). Finally, the melting temperature of refractory metal grains may have been at least partially below the liquidus temperature of some chondrules, meaning that some metal grains might not have been melted and, as such, might have become part of the matrix instead of being incorporated into the chondrules (Budde et al., 2016a, 2016b). Thus, although the exact mechanism remains uncertain, formation of chondrules by localized melting events in the disk can account for the observed isotopic complementarity of chondrules and matrix.

The formation of chondrules from a spatially restricted reservoir of solar nebula dust also provides a mechanism for keeping chondrules and matrix together. If chondrules and matrix from a given chondrite originated from the same reservoir of dust, and provided that no material was lost from this reservoir after chondrule formation and before chondrite accretion, then the bulk chondrite would naturally have the same isotopic composition as the original reservoir from which the chondrules and matrix derive. A corollary of this is that to avoid loss of either chondrules or matrix, there probably was a strong temporal link between chondrule formation and chondrite accretion (see Section 10.4). Alexander and Ebel (2012) argued that in a turbulent solar nebula, chondrules would rapidly mix on timescales of <1 Ma and on this basis inferred that the distinct physical and chemical properties of chondrules from a given chondrite group could not be preserved, unless chondrules rapidly accreted into planetesimals. Nevertheless, Jacquet et al. (2012) argued that immediate chondrite accretion following chondrule formation may not be necessary to preserve chondrule-matrix complementarity, provided that solids and gas are tightly coupled to each other. Under these conditions, more complex accretion histories might be possible, in which chondrites consist of several distinct dust populations (each consisting of chondrules and matrix) that could, in principle, have formed over an extended period of time (Goldberg et al., 2015). However, these models provide no precise estimate for the timescale over which chondrule-matrix complementarity could be preserved, preventing significant tightening of constraints on a possible time gap between chondrule formation and chondrite accretion in these models. We, therefore, stress that by far the most straightforward way of preserving complementarity is the immediate accretion of chondrules and matrix into a parent body. In this case, no special conditions need to be invoked to preserve distinct dust populations for an extended period of time.

The derivation of chondrules and matrix from a single reservoir of dust raises the question of whether this implies complete chemical or thermal processing of matrix during chondrule formation. Evidently this was not the case because the matrix contains presolar grains and thus has, at least in part, never been heated significantly (e.g., Huss et al., 2003). Moreover,

Alexander (2005) argued that the matrices of all chondrites are dominated by CI-like material, also implying that matrix (at least significant parts of it) had not been significantly modified during chondrule formation. However, the complementarity does not require thermal processing of matrix; it only requires that the material that was removed from the chondrules (or the chondrule precursors) was incorporated into the matrix and was not lost. Thus, the evidence that matrix escaped thermal processing does not contradict the inference of complementarity that chondrules and matrix derive from a common reservoir of solar nebula dust.

In summary, of the different models proposed for the origin of chondrules, only models in which chondrules are the result of localized melting events in the solar protoplanetary disk are consistent with the isotopic complementarity of chondrules and matrix. Other models, such as the *x*-wind model as well as the splashing and impact jetting models, cannot account for some or all of the constraints derived from the isotopic complementarity.

10.3.4 Significance of Isotope Anomalies in Single Chondrules

One important implication of chondrule-matrix complementarity is that chondrules from a given chondrite group should all derive from spatially restricted areas of the disk. However, variations in ^{54}Cr isotopic compositions of individual chondrules from CV chondrites have been interpreted to reflect formation at different orbital distances, followed by transport of chondrules across the disk before accretion to the CV parent body (Olsen et al., 2016). This interpretation is based on the observation that the range of ^{54}Cr compositions observed among CV chondrules is similar to the range of ^{54}Cr compositions for bulk meteorites. Obviously, such a disk-wide transport of chondrules is inconsistent with the formation of chondrules in localized regions as inferred from the isotopic complementarity. However, it is important to note that the ^{54}Cr data cannot be used to distinguish between transport of chondrules and transport of chondrule *precursors*. As such, the ^{54}Cr signatures do not provide evidence that chondrules themselves formed in different regions of the disk; they only show that chondrules formed from isotopically heterogeneous precursors. This heterogeneity may have arisen locally within the disk, or may reflect transport of isotopically anomalous dust grains across the disk, followed by incorporation of these dust grains into chondrule precursors, which then later melted to form chondrules.

Direct evidence for such transport processes comes from Ti isotopic data for chondrules. As for ^{54}Cr, individual CV chondrules also display a wide range of ^{50}Ti isotopic compositions. Gerber et al. (2017) demonstrated that the ^{50}Ti variations reflect the variable admixture of CAI-like and ^{50}Ti-enriched material to the chondrules. The ^{50}Ti variations, therefore, reflect a 'nugget' effect arising from the incorporation of isotopically anomalous grains into chondrule precursors, rather than providing a unique signature of distinct formation locations in the disk. The variable ^{54}Cr compositions of CV chondrules are thus most likely also due to a nugget effect, reflecting the incorporation of ^{54}Cr-rich dust grains into chondrule precursors (Gerber et al., 2017). As such there is no need to invoke disk wide transport of chondrules to account for their variable ^{54}Cr compositions, and the ^{54}Cr (and ^{50}Ti) anomalies in CV chondrules are consistent with formation in localized regions of the disk, as required by the isotopic complementarity of CV chondrules and matrix.

10.4 Hf–W Chronology of CV and CR Chondrules

10.4.1 ^{182}Hf–^{182}W Ages

The Hf–W system can be used to date chondrules, because chondrule formation and associated metal-silicate fractionation led to substantial Hf–W fractionation among the constituents of primitive chondrites. For instance, in the CV3 chondrite Allende, chondrules have elevated Hf/W ratios, while matrix is characterized by correspondingly low Hf/W ratios (Becker et al., 2015; Budde et al., 2016b). In CR chondrites, chondrules typically contain metal and for these samples the major Hf–W fractionation therefore is between silicates and metal (Budde et al., 2018).

The Hf–W system cannot easily be applied to single chondrules, because the W concentrations in chondrules are too low for precise isotope analysis (chondrules contain ~90 ng/g W, but ~30 ng W are needed for precise W isotopic analysis). The Hf–W data are, therefore, typically obtained on pooled chondrule separates, each consisting of hundreds to thousands of chondrules or chondrule fragments (Budde et al., 2016b, 2018). To date, there are two precise Hf–W ages for primitive carbonaceous chondrites. Chondrules and matrix samples from the CV3 chondrite Allende define a Hf–W isochron that corresponds to an age of 2.2 $\pm$ 0.8 Ma after CAI formation at 4,567.3 Ma (Figure 10.4a) (Budde et al., 2016b), and metal and silicate fractions from four CR2 chondrites define a Hf–W isochron with an age of 3.6 $\pm$ 0.6 Ma after CAI formation (Figure 10.4b) (Budde et al., 2018). Of note, an isochron regression using only data for silicate and metal fractions separated from CR chondrules (Figure 10.4c) yields the same age as the combined isochron for bulk metal and silicate fractions. This is consistent with the idea that the major metal-silicate fractionation in CR chondrites was associated with chondrule formation (e.g., Kong et al., 1999; Campbell et al., 2005; Jacquet et al., 2013).

It has been suggested that the Hf–W ages are not chronologically meaningful, because the very presence of nucleosynthetic W isotope anomalies would mean that there had been no W isotopic equilibration among the components used to construct the Hf–W isochrons (Chapter 11). However, the presence of nucleosynthetic isotope anomalies by no means excludes or requires that chondrules, matrix, and metal were not in Hf–W isotopic equilibrium. This is because the nucleosynthetic isotope anomalies arise from the heterogeneous distribution of small presolar grains with very large isotopic anomalies. As such, the presolar grains contain a negligible amount of the bulk W present in chondrules and matrix, meaning that the heterogeneous distribution of presolar grains has no effect on the chemical fractionation and equilibration of Hf and W between chondrules and matrix (or metal). In other words, the nucleosynthetic W isotope anomalies simply reflect the complementary depletion and enrichment of presolar grains between two components that otherwise were in isotopic equilibrium. Moreover, as noted above (sect. 10.2.1), nucleosynthetic W isotope anomalies are very small for the ^{182}W/^{183}W ratio normalized to ^{186}W/^{183}W. Thus, using these data in the isochron regression makes it possible to assess whether there had been any primordial W isotopic heterogeneity unrelated to the nucleosynthetic W isotope variations. Of note, the ^{182}W/^{183}W data (normalized to ^{186}W/^{183}W) provide precise isochrons for both Allende chondrules and matrix as well as for CR metal and silicates. This demonstrates that there was no initial W isotopic heterogeneity (other than the nucleosynthetic variations) among the components used to define the isochrons. Thus, the Hf–W data define meaningful isochrons.

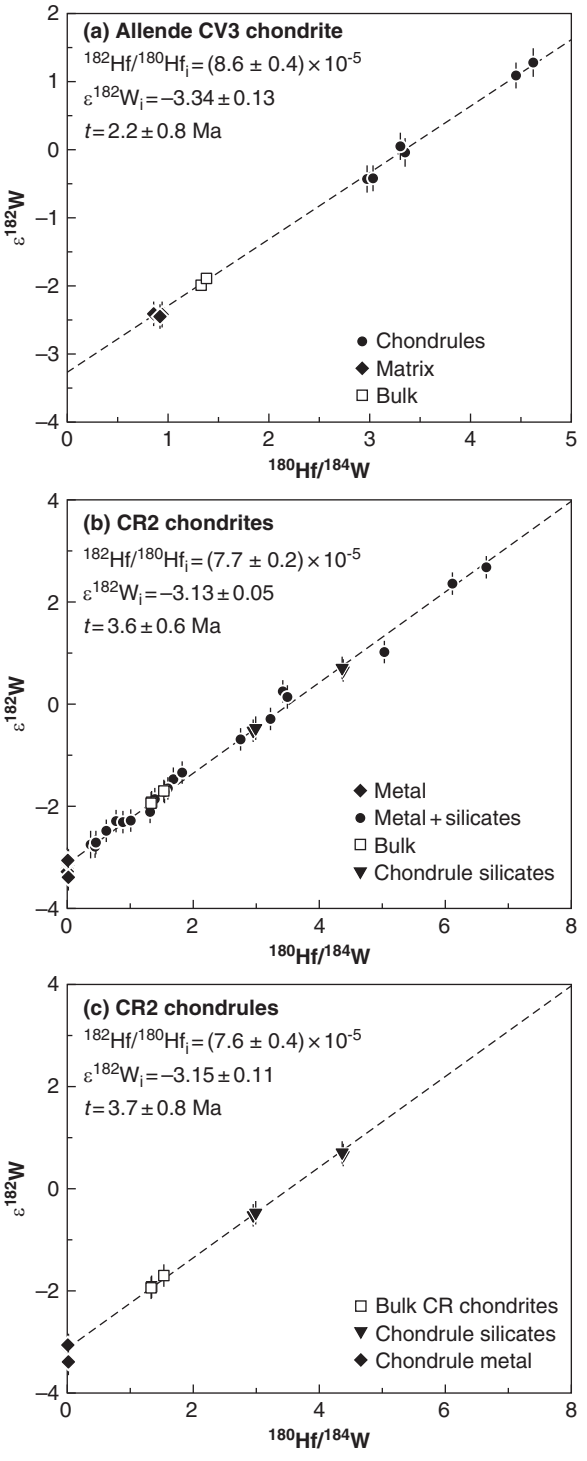

Figure 10.4 Hf–W isochrons for CV and CR chondrites. Ages calculated using the initial $^{182}Hf/^{180}Hf$ obtained from the isochrons and equation 1. (a) Allende chondrules and matrix. Data from Budde et al. (2016b). (b) Metal and silicate fractions from four different CR chondrites, and (c) metal and silicate fractions from chondrules of CR chondrites. Data for CR chondrites from Budde et al. (2018).

10.4.2 Comparison to ^{26}Al–^{26}Mg Ages

The Hf–W ages for CV and CR chondrules are in very good agreement with Al–Mg ages reported for these two groups of chondrites. For CV chondrites, the Al–Mg system in chondrules might be partially or wholly reset during parent body alteration (Alexander and Ebel, 2012), but Nagashima et al. (2017) argued that for the least metamorphosed CV chondrite Kaba, the Al–Mg system has not been disturbed. For Kaba chondrules, these authors reported an initial $^{26}Al/^{27}Al = (4.8 \pm 2.1) \times 10^{-6}$, corresponding to an Al–Mg age of 2.4 ± 0.4 Ma after CAI formation [using $^{26}Al/^{27}Al = (5.23 \pm 0.13) \times 10^{-5}$ for CAIs; Jacobsen et al., 2008]. This Al–Mg age for Kaba chondrules is in excellent agreement with the Hf–W age of 2.2 ± 0.8 Ma for Allende chondrules and matrix. Schrader et al. (2017) showed that the initial $^{26}Al/^{27}Al$ of CR chondrules is significantly lower than those in chondrules from other chondrite groups, and also showed that this lower initial $^{26}Al/^{27}Al$ does not reflect disturbance and resetting by parent body processes. These authors reported a weighted average initial $^{26}Al/^{27}Al = (1.33 \pm 0.29) \times 10^{-6}$ for CR chondrules, corresponding to an Al–Mg age of 3.8 ± 0.2 Ma after CAI formation. Again, this age is in excellent agreement with the Hf–W age for CR chondrules of 3.6 ± 0.6 Ma after CAIs.

The good agreement of Hf–W and Al–Mg ages for CV and CR chondrules not only demonstrates that these formation ages for chondrules are robust, but also has important implications for assessing the distribution of ^{26}Al in the solar nebula. Although the Al–Mg system can provide very precise ages for early Solar System objects, differences in inferred initial $^{26}Al/^{27}Al$ ratios could potentially also reflect the heterogeneous distribution of ^{26}Al in the solar nebula, rather than different formation times. For instance, on the basis of correlated ^{54}Cr and ^{26}Mg anomalies in bulk meteorites and CAI, Larsen et al. (2011) argued for a high degree of $^{26}Al/^{27}Al$ heterogeneity of up to ~80 percent, in which case the Al–Mg system could not be used as a chronometer. However, the ^{26}Mg variations more likely reflect small nucleosynthetic Mg isotope anomalies and not large-scale $^{26}Al/^{27}Al$ heterogeneity (Kruijer et al., 2014a). Nevertheless, for a reliable chronological interpretation of Al–Mg data it is important to independently evaluate the level of $^{26}Al/^{27}Al$ homogeneity/heterogeneity.

To assess the chronological significance of Al–Mg ages it is useful to compare them to ages obtained from other chronometers, such as the Hf–W system. Such a comparison can be made for bulk CAIs, CV, and CR chondrules as well as angrites (basaltic achondrites), because for all these samples precise Al–Mg and Hf–W data are available. Moreover, these samples formed over almost the entire lifetime of ^{26}Al (i.e., within the first ~5 Ma of the Solar System), making it possible to evaluate possible heterogeneities in $^{26}Al/^{27}Al$ at different times of Solar System evolution. Figure 10.5 illustrates that the Al–Mg and Hf–W ages of the aforementioned samples are concordant. The good agreement between ages of four different samples that formed at different times and in different areas of the protoplanetary disk provides strong evidence for a homogeneous distribution of ^{26}Al at the scale of bulk CAIs and bulk meteorites. Nevertheless, owing to the much shorter half-life of ^{26}Al compared to ^{182}Hf, small $^{26}Al/^{27}Al$ heterogeneities may still exist that could not be resolved by age comparison to the Hf–W system. Taking the scatter around the correlation in Figure 10.5 as a measure of the permissible degree of $^{26}Al/^{27}Al$ heterogeneity limits it to smaller than ~10–20 percent (Budde et al., 2017). Note that this value only provides a maximum estimate and by no means indicates or requires an actual heterogeneity in the distribution of ^{26}Al. As such, these data demonstrate that Al–Mg ages for chondrules and other samples have chronological significance.

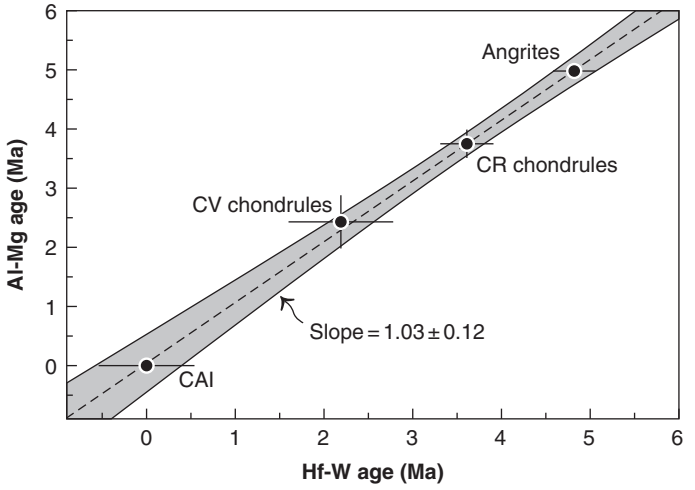

Figure 10.5 Comparison of Al–Mg and Hf–W ages for different meteorites. All ages are calculated relative to CAIs, but excluding the uncertainty on the initial $^{182}Hf/^{180}Hf$ and $^{26}Al/^{27}Al$ ratios of the CAIs. This was done to use CAIs as an independent data point in the age comparison. For data sources, see Budde et al. (2018).

10.4.3 Comparison to ^{207}Pb–^{206}Pb Ages

The Hf–W ages for the CV and CR chondrules are also in good agreement with the average Pb–Pb ages reported for chondrules from these two chondrite groups. For multi-chondrule fractions from Allende, Pb–Pb ages of 4,565.6 ± 1.0 Ma (Amelin and Krot, 2007), 4,564.5 ± 0.5 Ma (Connelly et al., 2008) and 4,564.3 ± 0.8 Ma (Connelly and Bizzarro, 2009) were reported. Note that these ages were corrected for age bias induced by differences in U isotopic compositions, as summarized in Brennecka et al. (2015). These Pb–Pb ages correspond to age differences relative to CAIs of 1.7 ± 1.0 Ma, 2.8 ± 0.5 Ma and 3.0 ± 0.8 Ma and as such are in good agreement with the Hf–W age of 2.2 ± 0.8 Ma of Allende chondrules and matrix. Amelin et al. (2002) reported a Pb–Pb age for a multi-chondrule fraction from a CR chondrite, which after correction for the U isotopic composition of CR chondrites, is 4,563.6 ± 0.6 Ma or 3.7 ± 0.6 Ma after CAI formation (Schrader et al., 2017). Again, this age is in very good agreement with the Hf–W age of 3.6 ± 0.6 Ma for metal-silicate fractionation in CR chondrites. Thus, for multichondrule fractions of CV and CR chondrules there is very good agreement between the Hf–W and Pb–Pb ages.

Matters become more complicated when Pb–Pb ages for individual chondrules are also considered. Connelly et al. (2012) reported Pb–Pb ages of 4,567.3 ± 0.4 Ma (i.e., 0.0 ± 0.4 Ma after CAIs) and 4,566.2 ± 0.6 Ma (i.e., 1.1 ± 0.6 Ma after CAIs) for two chondrules from the CV chondrite Allende. Of note, both ages are older than the aforementioned Pb–Pb ages determined for multi-chondrule separates from Allende. More recently, Bollard et al. (2017) reported Pb–Pb ages for chondrules from ordinary and CR chondrites, some of which also seem to be as old as CAI. On this basis, both Connelly et al. (2012) and Bollard et al. (2017) argued that chondrules formed continuously over at least the first ~3 Ma of the Solar System.

Such an extended formation period for chondrules from a single chondrite group is not apparent in the Al–Mg ages for chondrules, however. For instance, chondrules from the CV chondrite Kaba all have indistinguishable Al–Mg ages, with a mean age of 2.4 ± 0.4 Ma after CAIs (Nagashima et al., 2017). As noted above, Kaba is one of the least metamorphosed CV chondrites and has been classified as petrologic type 3.1 (Bonal et al., 2006); as such the Al–Mg systematics of chondrules from Kaba should have remained largely undisturbed as a result of parent body metamorphism. For other, more strongly metamorphosed CV chondrites (e.g., Allende, petrologic type 3.6; Bonal et al., 2006) the Al–Mg chondrule ages are more variable and, compared to chondrules from Kaba, extend to younger apparent ages. However, this range of ages reflects disturbance of the Al–Mg system during parent body metamorphism and *not* an extended period of chondrule formation (Nagashima et al., 2017). The duration of CV chondrule formation as derived from Al–Mg ages can therefore only be reliably deduced from the least metamorphosed sample (in this case, Kaba). As such, the Al–Mg data for Kaba indicate that CV chondrules formed within a time interval of <1 Ma.

The Al–Mg age distributions of individual chondrules from other chondrite groups show that in general the majority of chondrules from a given group formed in a narrow time interval. For instance, although Villeneuve et al. (2009) identified several peaks in the Al–Mg age distribution of chondrules from primitive ordinary chondrites, ~80 percent of these chondrules formed in a time interval between ~1.5 and ~2.8 Ma after CAIs. Likewise, Schrader et al. (2017) observed that ~90 percent of chondrules from CR chondrites formed at ~3.5 Ma after CAIs. It is noteworthy that the true range of formation ages for chondrules from a given chondrite might be smaller than the reported range of Al–Mg ages, because the Al–Mg system might be partially disturbed by parent body processes (Alexander and Ebel, 2012) and because the observed range in ages at least in part reflects analytical uncertainties and not a true range in formation ages. Thus, taken together, the Al–Mg data indicate that the vast majority of chondrules from a given chondrite formed in a narrow time interval of <1 Ma.

The discrepancy between this short interval of <1 Ma obtained from Al–Mg data and the extended period of ~3 Ma deduced from the Pb–Pb ages cannot reflect a heterogeneous distribution of ^{26}Al at the scale of individual chondrules. This is because ^{26}Al/^{27}Al heterogeneity among the precursor material of individual chondrules would lead to an apparent range in ages and not to one consistent age. The discrepancy between the Al–Mg and Pb–Pb ages also cannot reflect a reduced initial ^{26}Al/^{27}Al of bulk chondrites. For instance, to account for the mismatch of Pb–Pb and Al–Mg ages for chondrules from ordinary and CR chondrites, Bollard et al. (2017) argued that at the time of CAI formation chondrule precursors had a lower initial ^{26}Al/^{27}Al of ~1 × 10^{-5} than CAIs themselves (^{26}Al/^{27}Al ~5 × 10^{-5}). This reduced initial ^{26}Al/^{27}Al would make the chondrule Al–Mg ages appear ~2 Ma too young. However, this possibility is effectively being ruled out by the good agreement of Al–Mg and Hf–W ages of CV and CR chondrules, angrites and CAIs (see above and Figure 10.5), demonstrating that the initial ^{26}Al/^{27}Al ratios of these samples are consistent with radioactive decay from a common Solar System initial value as measured in CAIs. Thus, the mismatch between Al–Mg and Pb–Pb ages for individual chondrules cannot be accounted for by a heterogeneous distribution of ^{26}Al, meaning that the Al–Mg data support neither the range of Pb–Pb ages observed for chondrules for a given chondrite group, nor the presence of chondrules as old as CAI.

The observation that some CV chondrules have apparent Pb–Pb ages as old as CAI is also difficult to reconcile with other chronological data for CV chondrites. This is because if there were a significant fraction of CV chondrules as old as CAI, then there must also be a significant fraction of much younger chondrules with ages of around ~4–5 Ma after CAIs. This is necessary to account for the Pb–Pb and Hf–W ages of between ~2 and ~3 Ma after CAIs obtained for multi-chondrule separates from Allende. However, there are no CV chondrules with reported formation ages as young as ~4–5 Ma after CAIs. Moreover, such young formation ages of CV chondrules would be inconsistent with independent constraints on the timing of parent body accretion and alteration. Secondary fayalites in CV chondrites, which formed during aqueous alteration on the parent body, have a ^{53}Mn–^{53}Cr age of 4.2 ± 0.8 Ma after CAIs (Doyle et al., 2015; Jogo et al., 2017). As chondrule formation obviously must predate aqueous alteration on the parent body, the Mn–Cr age of secondary fayalites effectively rules out that CV chondrules could have formed as late as 4–5 Ma after CAIs. Moreover, to facilitate heating and formation of aqueous fluids that ultimately lead to alteration, there must be a time gap between chondrule formation (and hence chondrite accretion) and parent body alteration. Using thermal modeling of asteroids heated internally by ^{26}Al decay, it has been shown that to account for the formation conditions and ages of secondary fayalites, the CV parent body must have accreted between ~2.5 Ma and ~3.3 Ma after CAI formation (Doyle et al., 2015; Jogo et al., 2017). On this basis, there should be no CV chondrules that formed later than ~3 Ma after CAIs and, consequently, only a very minor fraction if any of CV chondrules can be as old as CAIs.

Finally, the formation of CV chondrules over an extended period of ~3 Ma as inferred from Pb–Pb chronometry is difficult to reconcile with the isotopic complementarity of chondrules and matrix. As argued above, this complementarity is most easily explained by rapid accretion of both chondrules and matrix into a chondrite parent body. This rapid accretion would also allow for the preservation of distinct chondrule populations, which is necessary to account for the distinct chemical and physical properties of chondrules from a given chondrite group (Alexander and Ebel, 2012).

In summary, the isotopic complementarity of chondrules and matrix, the narrow range of Al–Mg ages of <1 Ma for chondrules from a given chondrite group, the good agreement of Al–Mg and Hf–W ages for chondrules, and the chronology of aqueous alteration on the CV chondrite parent body combined with constraints on the time of parent body accretion, all indicate that the vast majority of chondrules for a single chondrite group formed in a narrow interval of time and that chondrule formation and chondrite accretion were about coeval. By contrast, the prolonged interval of chondrule formation inferred from Pb–Pb chronometry is inconsistent with all these constraints. As such, the variable Pb–Pb ages reported for chondrules from a given chondrite group either do not reflect true differences in chondrule formation ages, or, alternatively, the Pb–Pb ages have been obtained on a set of chondrules that represents only a very minor fraction of the entire population of chondrules.

10.5 Hf–W Chronology of Ordinary Chondrites

Ordinary chondrites contain abundant metal and as such can be well dated using the Hf–W system through metal-silicate isochrons. To date, the Hf–W system has been applied to several

equilibrated ordinary chondrites of petrologic types 4 to 6 (Kleine et al., 2008; Hellmann et al., 2017). As the Hf–W closure temperature is similar to the estimated peak metamorphic temperatures of ordinary chondrites, the Hf–W ages closely approximate the time of the thermal peak for each sample (Kleine et al., 2008). As such, the Hf–W ages provide insights into the high-temperature thermal evolution of ordinary chondrites, information that is critical for assessing the heat source for metamorphism and the internal structure of ordinary chondrite parent bodies.

The Hf–W ages for type 4 ordinary chondrites typically are ~3–4 Ma, while type 5 and 6 chondrites have ages of between ~6 and ~12 Ma, post CAI formation (Figure 10.6). This range in ages is consistent with the expected timescale of thermal metamorphism in asteroids that accreted at ~2 Ma after CAI formation and were internally heated by decay of ^{26}Al (Trieloff et al., 2003; Kleine et al., 2008; Henke et al., 2012). Of note, this timescale of parent body accretion is consistent with Al–Mg ages for chondrules from primitive ordinary chondrites (Kita et al., 2000; Rudraswami and Goswami, 2007; Villeneuve et al., 2009), indicating that

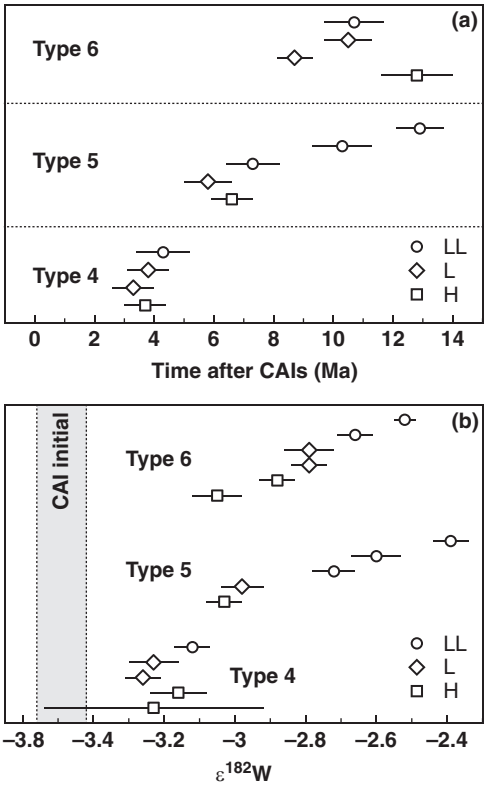

Figure 10.6 (a) Hf–W ages and (b) initial ε^{182}W of ordinary chondrites. Note that for a given petrologic type, there are no systematic differences between the Hf–W ages for H, L, and LL chondrites. By contrast, metal from type 5 and 6 LL chondrites always has higher ε^{182}W compared to H and L metals of the same petrologic type. Data from Hellmann et al. (2017).

there was a close temporal link between chondrule formation and chondrite accretion (see also Section 10.6).

The H, L, and LL subgroups of ordinary chondrites are distinguished based on different metal contents, most likely as a result of metal-silicate fractionation prior to parent body accretion. Of note, whereas for all three subgroups metal samples from type 4 samples have similar and comparatively low $\varepsilon^{182}W$ (providing the initial ^{182}W composition at the time of Hf–W closure), samples of higher petrologic types (type 5 and 6) exhibit higher and also more variable initial $\varepsilon^{182}W$ values (Figure 10.6). As samples of a given petrologic type from the H, L, and LL subgroups have similar Hf–W ages, their different initial $\varepsilon^{182}W$ cannot reflect different times of Hf–W closure. Instead they reflect distinct Hf/W ratios of the H, L, and LL parent bodies, which over time led to the observed variations in initial $\varepsilon^{182}W$. The highest initial $\varepsilon^{182}W$ are observed for type 5 and 6 LL chondrites, while H chondrites of similar age have much lower initial $\varepsilon^{182}W$ (Figure 10.6). The H chondrites therefore evolved with the lowest and LL chondrites with the highest Hf/W. Hellmann et al. (2017) demonstrated that these distinct Hf/W ratios were established between 1.5 and 3 Ma after CAI formation. A fractionation earlier than ~1.5 Ma can be excluded because in this case the type 4 ordinary chondrites would already have had distinct initial $\varepsilon^{182}W$ values, and because the back projection of the $\varepsilon^{182}W$ composition of type 4 metal from L and LL chondrites would result in $\varepsilon^{182}W$ values below the solar system initial value defined by CAIs. A fractionation later than ~3 Ma can also be excluded because the Hf–W fractionation among the different subgroups cannot postdate the onset of thermal metamorphism in each of the bodies, as given by the Hf–W ages for type 4 chondrites (Figure 10.6).

The metal-silicate fractionation among the different subgroups of ordinary chondrites at 1.5–3 Ma after CAIs was about coeval with formation of ordinary chondrite chondrules at ~2 Ma, consistent with the idea that chondrule formation was associated with metal-silicate fractionation. It is noteworthy that H chondrites have the same Fe/Si (and hence metal-to-silicate) ratio as CI chondrites (Palme et al., 2014), implying that the Hf/W ratio of H chondrites reflects the average ratio prior to metal-silicate fractionation among the ordinary chondrite subgroups. If this is correct, then metal must have been removed from L and LL chondrites, to accommodate their higher Hf/W. Of note, the aerodynamic properties of metal in ordinary chondrites are most similar to those of chondrules from H chondrites (Jacquet, 2014), suggesting that aerodynamic sorting did not significantly affect the chondrule-to-metal ratio in H chondrites. By contrast, in L and LL chondrites, chondrules might have been fractionated from metal grains. Thus, the distinct metal-silicate ratios of the ordinary chondrite subgroups probably reflect varying degrees of metal loss, possibly by aerodynamic sorting from H chondrite-like precursors.

10.6 Chondrules and the Accretion of Planetesimals

Chondrite parent bodies underwent different thermal histories, ranging from high temperature thermal metamorphism in ordinary chondrite parent bodies to the much lower temperature aqueous alteration typical for many carbonaceous chondrites (e.g., Huss et al., 2006; Krot et al., 2006). Figure 10.7 shows that there is an inverse correlation between chondrule ages and peak temperatures inferred for each chondrite parent body. For instance, chondrules from ordinary

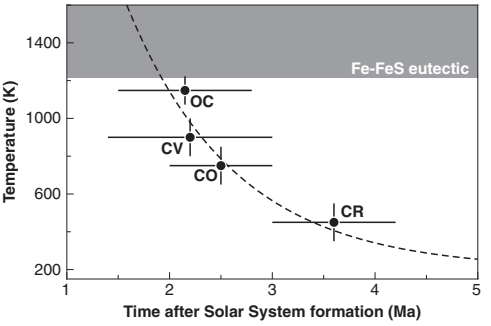

Figure 10.7 Peak temperature reached inside chondrite parent bodies versus chondrule ages. Whereas the ages for OC and CO chondrules are Al–Mg ages (Kurahashi et al., 2008; Villeneuve et al., 2009), the ages shown for CV and CR chondrules are Hf–W ages. As discussed in the text, there is very good agreement between the Hf–W and Al–Mg ages for these chondrites. The dashed line is the maximum temperature increase through decay of ^{26}Al, calculated by assuming the Al concentration of 1.167 wt. % of H chondrites (Wasson and Kallemeyn, 1988). These calculations only serve to illustrate that the observed thermal histories of chondrites are consistent with the effects expected from heating through ^{26}Al decay at different times of parent body accretion. In reality, the thermal evolution of chondrite parent bodies is more complex. Estimated peak temperatures for the different chondrite groups taken from Scott (2007). The gray box shows the temperature field in which melting will occur, indicating that bodies accreted within the first ~2 Ma of the solar system underwent at least partial melting.

chondrites are about ~1–2 Ma older than chondrules from CR chondrites, and peak metamorphic temperatures estimated for ordinary chondrite parent bodies were much higher (up to ~1,200 K) than those for the CR chondrite parent body (lower than ~500 K). This inverse correlation between chondrule ages and chondrite peak temperatures provides several important observations. First, such a correlation is expected only if the chondrule ages closely approximate the time of parent body accretion, defining the time at which heating inside the bodies started. Of note, this is consistent with the chronology of chondrule formation and independent constraints on the time of chondrite parent body accretion. For instance, based on Al–Mg chronometry, CV chondrules formed at 2.4 ± 0.4 Ma after CAIs, consistent with an ~2.5–3.3 Ma accretion age of the CV parent body derived from Mn–Cr dating of fayalites combined with thermal modeling (see Section 10.4). Similarly, the chronology of the thermal metamorphism of ordinary chondrites combined with thermal modeling provides an accretion age of ~2 Ma after CAIs for the ordinary chondrite parent bodies. Again, this is consistent with Al–Mg ages for chondrules from the most primitive ordinary chondrites (see Section 10.5). This close temporal link between chondrule formation and chondrite accretion is also consistent with the isotopic complementarity of chondrules and matrix (see Section 10.3).

Another important observation from Figure 10.7 is that the decay of ^{26}Al must have been the dominant heat source determining the thermal history of chondrite parent bodies. This is because ^{26}Al is the only heat source whose power strongly decreases as a function of accretion time. This suggests that, for instance, CR chondrites predominantly underwent aqueous alteration on their parent body not only because they contained water ice, but also because the CR chondrite parent body, owing to its late accretion, contained too little ^{26}Al for significant thermal metamorphism. Of note, the inverse correlation shown in Figure 10.7 in principle also

extends to differentiated meteorites. These derive from bodies that underwent large-scale melting and chemical differentiation, and, based on Hf–W chronometry, accreted within the first ~1 Ma of the Solar System (Kruijer et al., 2014b, 2017; Kleine and Walker, 2017). At this early time, ^{26}Al was sufficiently abundant to cause complete melting and efficient metal-silicate differentiation (Figure 10.7).

A final important observation from Figure 10.7 is that the oldest chondrule population (i.e., those from ordinary chondrites) formed at exactly the time when ^{26}Al had decayed to a level at which it can no longer cause melting and differentiation of planetesimals. This is unlikely to be coincidence but rather suggests that planetesimals that formed earlier than the ordinary chondrite parent bodies also contained chondrules initially, but that these chondrules were destroyed later during subsequent melting and differentiation. Thus, chondrule formation probably did not only commence at ~2 Ma after solar system formation, but started as soon as the earliest planetesimals formed. A corollary of this observation is that planetesimals in general might have contained chondrules, implying that chondrule formation was closely linked to, and might have even been a critical step towards, making planetesimals.

10.7 Conclusions

Tungsten isotope studies on chondrites and chondrite components have led to several major constraints that are key for understanding the origin of chondrules and chondrites:

- Chondrules and matrix (or metal) have complementary nucleosynthetic isotope anomalies, indicating that there is a strong genetic link between these three components.
- The isotopic complementarity reflects the uneven distribution of a metallic presolar carrier between chondrules and matrix (or metal), and as such most likely results from metal-silicate fractionation during chondrule formation.
- The complementarity is difficult to reconcile with an origin of chondrules by protoplanetary impacts and also with models in which chondrules and matrix formed in different regions of the protoplanetary disk (e.g., *x*-wind model). As such, the complementarity indicates that chondrules formed by localized melting of dust aggregates in the solar nebula.
- The isotopic complementarity is best explained by a rapid accretion of chondrules and matrix into a parent body. This is consistent with Hf–W and Al–Mg evidence that chondrules from a given chondrite group formed in a narrow time interval of $<$1 Ma, and implies a strong temporal link between chondrule formation and chondrite accretion. Such a link is also evident from the inverse correlation of chondrule ages and peak metamorphic temperatures reached inside chondrite parent bodies.
- Metal-silicate fractionation among subgroups of ordinary chondrites was about coeval to chondrule formation and may have occurred by aerodynamic sorting of chondrules (or their precursors) and metal grains. This provides further evidence that chondrule formation was associated with metal-silicate fractionation.
- CR chondrules formed significantly later than other chondrules (except for CB chondrules, which likely formed by a different formation mechanism than other chondrules; Chapter 2), implying that chondrule formation and accretion of planetesimals occurred for at least ~3–4 Ma after solar system formation.

- The good agreement of Hf–W and Al–Mg ages for several early solar system objects indicates a homogeneous distribution of ^{26}Al in the solar nebula, and limits any possible ^{26}Al/^{27}Al heterogeneity to less than 10–20 percent. The Al–Mg system can therefore be used as a precise chronometer for early Solar System processes.
- Decay of ^{26}Al was the dominant heat source determining the thermal history of planetesimals, including the parent bodies of both differentiated meteorites and chondrites.

Acknowledgments

We thank Emmanuel Jacquet and Graeme Poole for constructive reviews that have greatly improved the chapter. We also thank Sara Russell, Sasha Krot and Harold Connolly for organising the chondrule workshop in London, and for their assistance and support in the production of this chapter and the entire book. Funding by the Deutsche Forschungsgemeinschaft (DFG) is gratefully acknowledged.

References

Alexander, C. M. O'D. (2005). From supernovae to planets: The view from meteorites and interplanetary dust particles. In A. N. Krot, E. R. D. Scott, and B. Reipurth (Eds.), *Chondrites and the Protoplanetary Disk*, 972–1002. *Astronomical Society of the Pacific Conference Series*, 341. San Francisco, CA: Astronomical Society of the Pacific.

Alexander, C. M. O.'D., and Ebel, D. S. (2012). Questions, questions: Can the contradictions between the petrologic, isotopic, thermodynamic, and astrophysical constraints on chondrule formation be resolved? *Meteoritics & Planetary Science*, **47**, 1157–1175.

Amelin, Y., and Krot, A. N. (2007). Pb isotopic ages of the Allende chondrules. *Meteoritics & Planetary Science*, **42**, 1321–1335.

Amelin, Y., Krot, A. N., Hutcheon, I. D., and Ulyanov, A. A. (2002). Lead isotopic ages of chondrules and calcium-aluminum-rich inclusions. *Science*, **297**, 1678–1683.

Arlandini, C., Käppeler, F., and Wisshak, K. (1999). Neutron capture in low-mass asymptotic giant branch stars: Cross sections and abundance signatures. *Astrophysical Journal*, **525**, 886–900.

Asphaug, E., Jutzi, M., and Movshovitz, M. (2011). Chondrule formation during planetesimal accretion. *Earth and Planetary Science Letters*, **308**, 369–379.

Becker, M., Hezel, D. C., Schulz, T., Elfers, B. -M., and Münker, C. (2015). Formation timescales of CV chondrites from component specific Hf–W systematics. *Earth and Planetary Science Letters*, **432**, 472–482.

Bland, P. A., Alard, O., Benedix, G. K., et al. (2005). Volatile fractionation in the early solar system and chondrule/matrix complementarity. *Proceedings of the National Academy of Sciences of the United States of America*, **102**, 13755–13760.

Bollard, J., Connelly, J. N., Whitehouse, M. J., et al. (2017). Early formation of planetary building blocks inferred from Pb isotopic ages of chondrules. *Science Advances*, **3**, (8), e1700407.

Bonal, L., Bourot-Denise, M., Quirico, E., and Montagnac, G. (2006). Determination of the petrologic type of CV3 chondrites by Raman spectroscopy of included organic matter. *Geochimica et Cosmochimica Acta*, **70**, 1849–1863.

Brennecka, G. A., Budde, G., and Kleine, T., (2015). Uranium isotopic composition and absolute ages of Allende chondrules. *Meteoritics & Planetary Science*, **50**, 1995–2002.

Budde, G., Burkhardt, C., Brennecka, G. A., et al. (2016a). Molybdenum isotopic evidence for the origin of chondrules and a distinct genetic heritage of carbonaceous and non-carbonaceous meteorites. *Earth and Planetary Science Letters*, **454**, 293–303.

Budde, G., Kleine, T., Kruijer, T. S., Burkhardt, C., and Metzler, K. (2016b). Tungsten isotopic constraints on the age and origin of chondrules. *Proceedings of the National Academy of Sciences*, **113**, 2886–2891.

Budde, G., Kruijer, T. S., and Kleine, T. (2018). Hf–W chronology of CR chondrites: Implications for the timescales of chondrule formation and the distribution of ^{26}Al in the solar nebula. *Geochimica et Cosmochimica Acta*, **222**, 284–304.

Burkhardt, C., Kleine, T., Dauphas, N., and Wieler, R. (2012). Nucleosynthetic tungsten isotope anomalies in acid leachates of the Murchison chondrite: Implications for Hf–W chronometry. *The Astrophysical Journal Letters*, **753**, L6.

Burkhardt, C., Kleine, T., Oberli, F., et al. (2011). Molybdenum isotope anomalies in meteorites: Constraints on solar nebula evolution and origin of the Earth. *Earth and Planetary Science Letters*, **312**, 390–400.

Burkhardt, C., Kleine, T., Palme, H., et al. (2008). Hf–W mineral isochron for Ca,Al-rich inclusions: Age of the solar system and the timing of core formation in planetesimals. *Geochimica et Cosmochimica Acta*, **72**, 6177–6197.

Campbell, A. J., Zanda, B., Perron, C., et al. (2005). Origin and thermal history of Fe-Ni metal in primitive chondrites. In A. N. Krot (Ed.), *Chondrites and the Protoplanetary Disk*. pp. 407–431. *Astronomical Society of the Pacific Conference Series*, 341. San Francisco, CA: Astronomical Society of the Pacific.

Connelly, J. N., Amelin, Y., Krot, A. N., and Bizzarro, M. (2008). Chronology of the solar system's oldest solids. *The Astrophysical Journal Letters*, 675, L121.

Connelly, J. N., and Bizzarro, M. (2009). Pb–Pb dating of chondrules from CV chondrites by progressive dissolution. *Chemical Geology*, **259**, 143–151.

Connelly, J. N., Bizzarro, M., Krot, A. N., et al. (2012). The Absolute Chronology and Thermal Processing of Solids in the Solar Protoplanetary Disk. *Science*, **338**, 651–655.

Connolly, H. C., and Desch, S. J. (2004). On the origin of the "kleine Kügelchen" called Chondrules. *Chemie der Erde – Geochemistry*, **64**, 95–125.

Connolly, H. C., Huss, G. R., and Wasserburg, G. J. (2001). On the formation of Fe-Ni metal in Renazzo-like carbonaceous chondrites. *Geochimica et Cosmochimica Acta*, **65**, 4567–4588.

Doyle, P. M., Jogo, K., Nagashima, K., et al. (2015). Early aqueous activity on the ordinary and carbonaceous chondrite parent bodies recorded by fayalite. *Nature Communications*, **6**, 7444.

Ebel, D. S., Brunner, C., Konrad, K., et al. (2016). Abundance, major element composition and size of components and matrix in CV, CO and Acfer 094 chondrites. *Geochimica et Cosmochimica Acta*, **172**, 322–356.

Gerber, S., Burkhardt, C., Budde, G., Metzler, K., and Kleine, T. (2017). Mixing and transport of dust in the early solar nebula as inferred from titanium isotope variations among chondrules. *Astrophysical Journal Letters*, **841**, L17.

Hellmann, J. L., Kruijer, T. S., and Kleine, T. (2017). Constraining the timescale of solar nebula metal-silicate fractionation using Hf–W chronometry of ordinary chondrites. *48th Lunar and Planetary Science Conference*, abstract #2046.

Henke, S., Gail, H. P., Trieloff, M., Schwarz, W. H., and Kleine, T. (2012). Thermal history modelling of the H chondrite parent body. *Astronomy & Astrophysics*, **545**, A45.

Hezel, D. C., and Palme, H. (2010). The chemical relationship between chondrules and matrix and the chondrule matrix complementarity. *Earth and Planetary Science Letters*, **294**, 85–93.

Hezel, D. C., and Palme, H. (2008). Constraints for chondrule formation from Ca–Al distribution in carbonaceous chondrites. *Earth and Planetary Science Letters*, **265**, 716–725.

Hubbard, A. (2016a). Partitioning tungsten between matrix precursors and chondrule precursors through relative settling. *The Astrophysical Journal*, **826**, 151.

Hubbard, A. (2016b). Ferromagnetism and particle collisions: Applications to protoplanetary disks and the meteoritical record. *The Astrophysical Journal*, **826**, 152.

Huss, G. R., Meshik, A. P., Smith, J. B., and Hohenberg, C. M. (2003). Presolar diamond, silicon carbide, and graphite in carbonaceous chondrites: Implications for thermal processing in the solar nebula. *Geochimica et Cosmochimica Acta*, **67**, 4823–4848.

Huss, G. R., Rubin, A. E., and Grossman, J. N. (2006). Thermal metamorphism in chondrites. In D. S. Lauretta, and H. Y. McSween (Eds.), *Meteorites and the Early Solar System II*, 567–586. Tucson, AZ: University of Arizona Press.

Jacobsen, B., Yin, Q. -Z., Moynier, F., et al. (2008). ^{26}Al-^{26}Mg and ^{207}Pb-^{206}Pb systematics of Allende CAIs: Canonical solar initial ^{26}Al/^{27}Al ratio reinstated. *Earth and Planetary Science Letters*, **272**, 353–364.

Jacquet, E. (2014). Transport of solids in protoplanetary disks: Comparing meteorites and astrophysical models. *Comptes Rendus – Geoscience*, **346**, 3–12.

Jacquet, E., Paulhiac-Pison, M., Alard, O., et al. (2013). Trace element geochemistry of CR chondrite metal. *Meteoritics & Planetary Science*, **48**, 1981–1999.

Jacquet, E., Gounelle, M., and Fromang, S. (2012). On the aerodynamic redistribution of chondrite components in protoplanetary disks. *Icarus*, **220**, 162–173.

Jogo, K., Nakamura, T., Ito, M., et al. (2017). Mn–Cr ages and formation conditions of fayalite in CV3 carbonaceous chondrites: Constraints on the accretion ages of chondritic asteroids. *Geochimica et Cosmochimica Acta*, **199**, 58–74.

Johnson, B. C., Minton, D. A., Melosh, H. J., and Zuber, M. T. (2015). Impact jetting as the origin of chondrules. *Nature*, **517**, 339–341.

Kita, N. T., Nagahara, H., Togashi, S., and Morishita, Y. (2000). A short duration of chondrule formation in the solar nebula: Evidence from ^{26}Al in Semarkona ferromagnesian chondrules. *Geochimica et Cosmochimica Acta*, **64**, 3913–3922.

Kita, N. T., and Ushikubo, T. (2012). Evolution of protoplanetary disk inferred from ^{26}Al chronology of individual chondrules. *Meteoritics & Planetary Science*, **47**, 1108–1119.

Kleine, T., Mezger, K., Palme, H., Scherer, E., and Münker, C. (2005). Early core formation in asteroids and late accretion of chondrite parent bodies: Evidence from ^{182}Hf-^{182}W in CAIs, metal-rich chondrites and iron meteorites. *Geochimica et Cosmochimica Acta*, **69**, 5805–5818.

Kleine, T., Touboul, M., Bourdon, B., et al. (2009). Hf–W chronology of the accretion and early evolution of asteroids and terrestrial planets. *Geochimica et Cosmochimica Acta*, **73**, 5150–5188.

Kleine, T., Touboul, M., Van Orman, J. A., et al. (2008). Hf–W thermochronometry: Closure temperature and constraints on the accretion and cooling history of the H chondrite parent body. *Earth and Planetary Science Letters*, **270**, 106–118.

Kleine, T., and Walker, R. J. (2017). Tungsten isotopes in planets. *Annual Review of Earth and Planetary Sciences*, **45**, 389–417.

Kong, P., Ebihara, M. and Palme, H. (1999). Distribution of siderophile elements in CR chondrites: Evidence for evaporation and recondensation during chondrule formation. *Geochimica et Cosmochimica Acta*, **63**, 2637–2652.

Krot, A. N., Hutcheon, I. D., Brearley, A. J., Pravdivtseva, O., and Petaev, M. I. (2006). Timescales and settings for alteration of chondritic meteorites. In D. S. Lauretta and H. Y. McSween (Eds.), *Meteorites and the Early Solar System II*, 525–554. Tucson, AZ: University of Arizona Press.

Kruijer, T. S., Kleine, T., Fischer-Godde, M., Burkhardt, C., and Wieler, R. (2014a). Nucleosynthetic W isotope anomalies and the Hf–W chronometry of Ca-Al-rich inclusions. *Earth and Planetary Science Letters*, **403**, 317–327.

Kruijer, T. S., Touboul, M., Fischer-Godde, M., et al. (2014b). Protracted core formation and rapid accretion of protoplanets. *Science*, **344**, 1150–1154.

Kruijer, T. S., Burkhardt, C., Budde, G., and Kleine, T. (2017). Age of Jupiter inferred from the distinct genetics and formation times of meteorites. *Proceedings of the National Academy of Sciences*, **114**, 6712–6716.

Kurahashi, E., Kita, N. T., Nagahara, H., and Morishita, Y. (2008). ^{26}Al-^{26}Mg systematics of chondrules in a primitive CO chondrite. *Geochimica et Cosmochimica Acta*, **72**, 3865–3882.

Larsen, K. K., Trinquier, A., Paton, C., et al. (2011). Evidence for magnesium isotope heterogeneity in the solar protoplanetary disk. *The Astrophysical Journal Letters*, **L37**, L37.

Nagashima, K., Krot, A. N., and Komatsu, M. (2017). ^{26}Al–^{26}Mg systematics in chondrules from Kaba and Yamato 980145 CV3 carbonaceous chondrites. *Geochimica et Cosmochimica Acta*, **201**, 303–319.

Olsen, M. B., Wielandt, D., Schiller, M., Van Kooten, E. M. M. E., and Bizzarro, M. (2016). Magnesium and ^{54}Cr isotope compositions of carbonaceous chondrite chondrules – Insights into early disk processes. *Geochimica et Cosmochimica Acta*, **191**, 118–138.

Palme, H., Hezel, D. C., and Ebel, D. S. (2015). The origin of chondrules: Constraints from matrix composition and matrix-chondrule complementarity. *Earth and Planetary Science Letters*, **411**, 11–19.

Palme, H., Lodders, K., and Jones, A. (2014). Solar System Abundances of the Elements. In H. D. Holland and K. K. Turekian (Eds.), *Treatise on Geochemistry* (Second Edition), 15–36. Oxford: Elsevier.

Qin, L., Dauphas, N., Wadhwa, M., Masarik, J., and Janney, P. E. (2008a). Rapid accretion and differentiation of iron meteorite parent bodies inferred from ^{182}Hf-^{182}W chronometry and thermal modeling. *Earth and Planetary Science Letters*, **273**, 94–104.

Qin, L. P., Dauphas, N., Wadhwa, M., et al. (2008b). Tungsten nuclear anomalies in planetesimal cores. *Astrophysical Journal*, **674**, 1234–1241.

Render, J., Fischer-Gödde, M., Burkhardt, C., and Kleine, T. (2017). The cosmic molybdenum-neodymium isotope correlation and the building material of the Earth. *Geochemical Perspectives Letters*, **3**, 170–178.

Rudraswami, N. G., and Goswami, J. N. (2007). ^{26}Al in chondrules from unequilibrated L chondrites: Onset and duration of chondrule formation in the early solar system. *Earth and Planetary Science Letters*, **257**, 231–244.

Sanders, I. S., and Scott, E. R. D. (2012). The origin of chondrules and chondrites: Debris from low-velocity impacts between molten planetesimals? *Meteoritics & Planetary Science*, **47**, 2170–2192.

Scherstén, A., Elliott, T., Hawkesworth, C., Russell, S. S., and Masarik, J. (2006). Hf–W evidence for rapid differentiation of iron meteorite parent bodies. *Earth and Planetary Science Letters*, **241**, 530–542.

Schrader, D. L., Nagashima, K., Krot, A. N., et al. (2017). Distribution of ^{26}Al in the CR chondrite chondrule-forming region of the protoplanetary disk. *Geochimica et Cosmochimica Acta*, **201**, 275–302.

Scott, E. R. D. (2007). Chondrites and the protoplanetary disk. *Annual Review of Earth and Planetary Sciences*, **35**, 577–620.

Shu, F. H., Shang, H., and Lee, T. (1996). Toward an astrophysical theory of chondrites. *Science*, **271**, 1545–1552.

Trieloff, M., Jessberger, E. K., Herrwerth, I., et al. (2003). Structure and thermal history of the H-chondrite parent asteroid revealed by thermochronometry. *Nature*, **422**, 502–506.

Trinquier, A., Elliott, T., Ulfbeck, D., et al. (2009). Origin of nucleosynthetic isotope heterogeneity in the solar protoplanetary disk. *Science*, **324**, 374–376.

Van Orman, J. A., Cherniak, D. J., and Kita, N. (2014). Magnesium diffusion in plagioclase: Dependence on composition, and implications for thermal resetting of the ^{26}Al-^{26}Mg early solar system chronometer. *Earth and Planetary Science Letters*, **385**, 79–88.

Villeneuve, J., Chaussidon, M., and Libourel, G. (2009). Homogeneous distribution of Al-26 in the Solar System from the Mg isotopic composition of chondrules. *Science*, **325**, 985–988.

Vockenhuber, C., Oberli, F., Bichler, M., et al. (2004). New half-life measurement of ^{182}Hf: Improved chronometer for the early solar system. *Physical Review Letters*, **93**, article # 172501.

Wasson, J. T., and Kallemeyn, G. W. (1988). Compositions of chondrites. *Philosophical Transactions of the Royal Society of London Series A-Mathematical Physical and Engineering Sciences*, **325**, 535–544.

Zanda, B., Bourot-Denise, M., Perron, C., and Hewins, R. H. (1994). Origin and metamorphic redistribution of silicon, chromium, and phosphorus in the metal of chondrites. *Science*, **265**, 1846–1849.

Zook, H. A. (1981). On a new model for the generation of chondrules. *Lunar and Planetary Science Conference, XII*, 1242–1244. Abstract.